Contribution from the Department of Chemistry,
Northwestern University, Evanston, Illinois 60201

Synthesis, Structure, and Transport Properties of Ta_2NiSe_7 and Ta_2PtSe_7

Steven A. Sunshine and James A. Ibers*

Received May 23, 1986

The new layered ternary chalcogenides Ta_2NiSe_7 and Ta_2PtSe_7 have been prepared and characterized. These compounds crystallize in the monoclinic space group C_{2h}^3-$C2/m$ with four formula units in the cell (for Ta_2NiSe_7 a = 13.827 (3) Å, b = 3.482 (1) Å, c = 18.577 (4) Å, and β = 108.80 (1)° and for Ta_2PtSe_7 a = 13.954 (13) Å, b = 3.530 (3) Å, c = 18.694 (17) Å, and β = 109.28 (3)°, both at −150 °C). The layers are comprised of Ta atoms in octahedral and bicapped-trigonal-prismatic chalcogen environments and Ni or Pt atoms in octahedral sites. Each Ni or Pt atom is shifted from the center of the octahedron toward one apex, resulting in square-pyramidal coordination. The structure contains one Se–Se pair (d = 2.549 (3) Å for Ta_2NiSe_7 and d = 2.597 (4) Å for Ta_2PtSe_7) in each trigonal prism of Se atoms. The transport properties of Ta_2NiSe_7 reveal that this material is metallic (σ_{rt} = 310 Ω^{-1} cm^{-1}) and diamagnetic (χ_{rt} = −1.54 × 10^{-7} emu g^{-1}).

Introduction

Recently we have reported several new compounds in the Ta/Nb–Ni/Pd/Pt–S/Se systems.[1-6] Our interest in such compounds arises in part from the potential extension of the structural features and physical properties of the binary Ta/Nb–S/Se systems to new ternary materials. Indeed, many of the compounds we have reported (e.g., Ta_2NiQ_5,[4] Ta_2PdQ_6,[3] and $Nb_2Pd_xSe_5$;[2] Q = S, Se) exhibit layered structures similar to those of the MQ_2 compounds (M = Ta, Nb; Q = S, Se). Yet, none of these compounds contains chalcogen–chalcogen bonds, as are present in the MQ_3 structures. Since interesting transport properties such as charge density waves,[7] metal–insulator transitions,[8] and superconductivity[9] are present in the trichalcogenides, we have attempted to synthesize similar compounds in the ternary Ta–Ni/Pt–S/Se systems. In this paper we report the synthesis and structure of the compounds Ta_2MSe_7 (M = Ni, Pt) as well as the physical properties of the Ni compound. These compounds contain an Se–Se bond.

Experimental Section

Synthesis of Ta_2NiSe_7. The compound may be prepared by direct combination of the elements. A stoichiometric amount of the elements, Ta powder (AESAR 99.98%), Ni powder (Alfa 99.9%), and Se powder (Atomergic 99.999%), is sealed in an evacuated (~10^{-5} torr) silica tube. The tube is placed in a furnace and subjected to a temperature gradient (725–650 °C) with the charge in the hot zone. Within 7 days long flat gray-black crystals form throughout the tube. A slight excess of chalcogen (~1% by weight) aids in crystal growth. The use of I_2 or Br_2 as a transport agent has an adverse effect on the reaction and leads to the formation of $TaSe_3$. Anal (Galbraith Laboratories, Inc.). Calcd for Ta_2NiSe_7: Ta, 37.18; Ni, 6.03; Se, 56.79. Found: Ta, 36.82; Ni, 5.71; Se, 56.69.

Synthesis of Ta_2PtSe_7. This compound is prepared in the same manner as Ta_2NiSe_7 (with Pt powder (AESAR 99.9%) substituted for Ni powder). Crystal growth is slower for the Pt compound, and longer reaction times are needed (10–14 days). The crystals obtained are small (0.1–0.3 mm long) and exhibit a shiny gray-black luster. The use of transport agents has the same effect as described above. The composition Ta_2PtSe_7 is confirmed by satisfactory refinement of the X-ray crystal structure.

Physical Measurements. Four-probe single-crystal conductivity measurements along the needle axis, b, of Ta_2NiSe_7 were performed with the use of previously described procedures.[10] Magnetic susceptibility measurements were performed at 10 kG on a sample of ground crystals with a SHE 800 Series SQUID susceptometer.

Table I. X-ray Data Parameters for Ta_2NiSe_7 and Ta_2PtSe_7

	Ta_2NiSe_7	Ta_2PtSe_7
formula	Ta_2NiSe_7	Ta_2PtSe_7
mol wt	973.33	1109.71
space group	C_{2h}^3-$C2/m$	C_{2h}^3-$C2/m$
a, Å	13.827 (3)	13.954 (13)
b, Å	3.482 (1)	3.530 (3)
c, Å	18.577 (4)	18.694 (17)
β, deg[a]	108.80 (1)	109.28 (3)
vol, Å^3	846.13	869.30
Z	4	4
T, °C	−150[b]	−150[c]
radiation	graphite-monochromated Mo Kα_1 (λ(Kα_1) = 0.7093 Å)	
cryst shape	needle bound by {010}, {100}, {001}, {10$\bar{2}$}, {10$\bar{1}$}	needle bound by {010}, {100}, {001}
cryst vol, mm^3	5.09 × 10^{-5}	2.14 × 10^{-5}
linear abs coeff, cm^{-1}	574.5	700.2
transmission factors	0.449–0.622	0.409–0.754
detector aperture, mm	3.0 high by 2.5 wide, 17 cm from cryst	5.0 high by 4.2 wide, 32 cm from cryst
takeoff angle, deg	2.5	2.5
scan type	θ–2θ	θ–2θ
scan speed, deg min^{-1}	2[d] (0° < θ < 17.5°), 1.33 (17.5° < θ < 30.0°)	1[e]
bkgd counts	$^1/_4$ of scan range on each side of reflection	10 s on either side of reflection with rescan option
scan range, deg	1.0 below Kα_1 to 1.0 above Kα_2	0.8 below Kα_1 to 0.7 above Kα_2
λ^{-1} sin θ limits, Å^{-1}	0.0566–0.7049	0.0431–0.6510
θ limits, deg	2.30 ≤ θ(Mo Kα_1) ≤ 30.0	1.75 ≤ θ(Mo Kα_1) ≤ 27.5
data collected	$\pm h,\pm k,\pm l$, 2.30° ≤ θ ≤ 25.0°; $\pm hkl$, 25.0° ≤ θ ≤ 30.0°	$\pm h,\pm k,\pm l$, 1.75° ≤ θ ≤ 25.0°; $\pm hkl$, 25.0° ≤ θ ≤ 27.5°
p Factor for $\sigma(F_o^2)$	0.03	0.04
no. of unique data	1399	1108
unique data with $F_o^2 > 3\sigma(F_o^2)$	834	1172
$R(F^2)$	0.080	0.077
$R_w(F^2)$	0.103	0.099
R (on F for $F_o^2 > 3\sigma(F_o^2)$)	0.043	0.043
error in observn of unit wt, e^2	0.97	1.22

[a] Cell refinements constrained α and γ to 90°. [b] The low-temperature system for the Nonius CAD4 diffractometer is from a design by Prof. J. J. Bonnet and S. Askenazy and is commercially available from Sotorem, Z. T. de Vic, 31320 Castanet-Tolosan, France. [c] The low-temperature system for the Picker FACS-1 diffractometer is based on a design by: Huffman, J. C. Ph.D. Thesis, Indiana University, 1974. [d] Reflections with $\sigma(I)/I > 0.33$ were rescanned up to a maximum time of 2 min. [e] The Picker FACS-1 diffractometer was operated under the Vanderbilt disk-oriented system (Lenhert, P. G. *J. Appl. Crystallogr.* **1975**, *8*, 568–570).

Collection of X-ray Diffraction Data. Analysis of oscillation and Weissenberg photographs revealed that the crystals possess monoclinic symmetry and the systematic extinction hkl, $h + k = 2n + 1$, indicative of the space groups C_2^3-$C2$, C_s^3-Cm, and C_{2h}^3-$C2/m$. The centrosymmetric

(1) Keszler, D. A.; Ibers, J. A. *J. Solid State Chem.* **1984**, *52*, 73–79.
(2) Keszler, D. A.; Ibers, J. A.; Shang, M.; Lu, J. *J. Solid State Chem.* **1985**, *57*, 68–81.
(3) Keszler, D. A.; Squattrito, P. J.; Brese, N. E.; Ibers, J. A.; Shang, M.; Lu, J. *Inorg. Chem.* **1985**, *24*, 3063–3067.
(4) Sunshine, S. A.; Ibers, J. A. *Inorg. Chem.* **1985**, *24*, 3611–3614.
(5) Keszler, D. A.; Ibers, J. A. *J. Am. Chem. Soc.* **1985**, *107*, 8119–8127.
(6) Squattrito, P. J.; Sunshine, S. A.; Ibers, J. A. *J. Solid State Chem.*, in press.
(7) Wilson, J. A. *Phys. Rev. B: Condens. Matter* **1979**, *19*, 6456–6468.
(8) Meerschaut, A.; Guemas, L.; Rouxel, J. *J. Solid State Chem.* **1981**, *36*, 118–123.
(9) Haen, P.; Lapierre, F.; Monceau, P.; Nunez Regueiro, M.; Richard, J. *Solid State Commun.* **1978**, *26*, 725–730.
(10) Phillips, T. E.; Anderson, J. R.; Schramm, C. J.; Hoffman, B. M. *Rev. Sci. Instrum.* **1979**, *50*, 263–265.

0020-1669/86/1325-4355$01.50/0

Table II. Positional and Thermal Parameters for Ta_2NiSe_7 and Ta_2PtSe_7

Ta_2NiSe_7

atom[a]	x	y	z	B_{eq}, Å^2
Ta(1)	0.151 270 (72)	0	0.399 142 (51)	0.36 (2)
Ta(2)	0.228 901 (75)	0	0.089 761 (54)	0.58 (2)
Ni	0.689 72 (23)	0	0.209 30 (17)	0.58 (7)
Se(1)	0.366 27 (17)	0	0.012 96 (12)	0.45 (5)
Se(2)	0.562 24 (21)	0	0.294 83 (13)	0.86 (6)
Se(3)	0.581 03 (17)	1/2	0.137 03 (13)	0.57 (5)
Se(4)	0.846 69 (17)	0	0.173 53 (12)	0.65 (5)
Se(5)	0.019 39 (18)	1/2	0.418 33 (13)	0.56 (5)
Se(6)	0.198 98 (17)	0	−0.446 65 (12)	0.46 (5)
Se(7)	0.259 23 (17)	0	0.299 70 (12)	0.48 (5)

Ta_2PtSe_7

atom	x	y	z	B_{iso}, Å^2
Ta(1)	0.150 919 (73)	0	0.398 874 (51)	0.28 (2)
Ta(2)	0.231 065 (75)	0	0.091 873 (51)	0.32 (2)
Pt	0.688 086 (69)	0	0.207 920 (48)	0.31 (2)
Se(1)	0.360 37 (18)	0	0.011 77 (12)	0.40 (4)
Se(2)	0.565 67 (18)	0	0.293 87 (13)	0.44 (4)
Se(3)	0.574 46 (18)	1/2	0.127 19 (12)	0.40 (4)
Se(4)	0.851 87 (18)	0	0.171 62 (12)	0.50 (4)
Se(5)	0.023 16 (18)	1/2	0.419 09 (12)	0.39 (4)
Se(6)	0.200 37 (18)	0	−0.447 35 (12)	0.36 (4)
Se(7)	0.264 58 (18)	0	0.303 78 (12)	0.35 (4)

[a] All atoms are in Wyckoff position 4i and have point symmetry *m*.

group $C2/m$ was chosen since satisfactory agreement indices, $R = 0.054$ and 0.046 for Ta_2NiSe_7 and Ta_2PtSe_7, respectively, were obtained from averaging the absorption-corrected intensities of the Friedel pairs. Diffraction data were collected on needle-shaped crystals at −150 °C with an Enraf-Nonius CAD-4 diffractometer (Ta_2NiSe_7) or a Picker FACS-1 diffractometer (Ta_2PtSe_7). In both cases six standard reflections measured every 3 h showed no significant variation in intensity. Data collection parameters and crystallographic details are given in Table I.

Solution and Refinement of the Structures. For Ta_2NiSe_7 initial calculations were performed on a VAX 11/730 computer with the use of the TEXSAN programs.[11] All atomic positions were determined from an *E* map generated by the program MITHRIL.[12] The compound Ta_2PtSe_7 is isostructural with Ta_2NiSe_7. All subsequent calculations were performed on a Harris 1000 computer with programs standard for this laboratory. Conventional atomic scattering factors[13] were used, and anomalous dispersion corrections[14] were applied. An analytical absorption correction was applied,[15] and the nonunique data were averaged. For Ta_2NiSe_7 the final cycle of refinement was performed on F_o^2 with anisotropic thermal parameters for each atom. For Ta_2PtSe_7 the final cycle of refinement was performed on F_o^2 with isotropic thermal parameters. Attempts to refine all atoms with anisotropic thermal parameters led to negative U_{22} terms for some atoms. This may arise from a slight bend in the crystal along the needle axis (*b*). It is not an artifact of the absorption correction, as the same trend is observed for the data before correction. An analysis of F_o^2 as a function of F_o^2, $\lambda^{-1}\sin\theta$, and Miller indices reveals no unusual trends for either structure. A similar analysis as a function of χ does demonstrate poorer agreement for reflections at χ near 90° (near the horizontal) for Ta_2PtSe_7; again this may be the result of crystal quality. For both compounds the unexceptional thermal parameters are consistent with an ordered structure of stoichiometry Ta_2MSe_7. The final difference electron density maps reveal no features greater than 5% of the height of a Ta atom.

Final positional and equivalent isotropic thermal parameters or isotropic thermal parameters are given in Table II. Final anisotropic thermal parameters for Ta_2NiSe_7 and structure amplitudes for both structures are provided in Tables III and IV.[16]

Results

Description of the Structure. A view down the *b* axis of the structure of Ta_2MSe_7 (M = Ni, Pt) with the labeling scheme is given in Figure 1. These compounds possess a novel laminar structure with the layers extending parallel to the *c* axis. A drawing of one layer as viewed orthogonal to the *bc* plane is provided in Figure 2. Metrical details are given in Table V. Each slab is composed of three types of chains that run along the *b* axis (Figure 3). Each of these chains occurs four times in the unit cell, twice in each independent slab. One of the three chains (A, Figure 3) contains edge-sharing octahedra centered by Ta atoms, as in Ta_2NiSe_5[4] or 1T–$TaSe_2$.[17] The second chain (B, Figure 3) consists of edge-sharing octahedra with Ni or Pt atoms displaced from the centers of these octahedra to give square-pyramidal geometry about the metal atoms. The final chain (C, Figure 3) possesses Ta-centered bicapped trigonal prisms of Se atoms that share triangular faces along the *b* axis. The trigonal prisms contain an Se–Se bond ($d = 2.549$ (3) and 2.597 (4) Å for Ta_2NiSe_7 and Ta_2PtSe_7, respectively). This same geometry is seen in $TaSe_3$[18] and $FeNb_3Se_{10}$.[19,20] These Se–Se distances are in good agreement

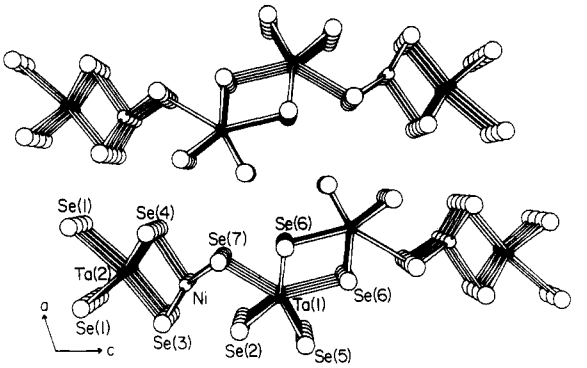

Figure 1. Perspective view of the Ta_2NiSe_7 structure down [010], showing the labeling scheme. The compound Ta_2PtSe_7 is isostructural. Here, and in Figure 2, small filled circles are Ta atoms, small open circles are Ni or Pt atoms, and large open circles are Se atoms.

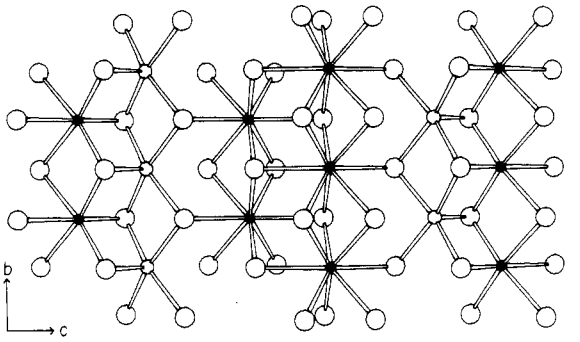

Figure 2. View of one slab of Ta_2MSe_7 in the *bc* plane.

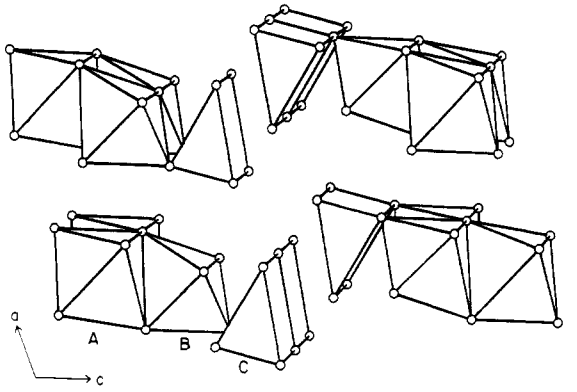

Figure 3. Polyhedral representation of the Ta_2MSe_7 structure: (A) Ta octahedra; (B) Ni or Pt octahedra; (C) Ta trigonal prisms.

(11) "Texsan, Texray Structure Analysis Package", Molecular Structure Corp. College Station, TX.
(12) Gilmore, C. J. *J. Appl. Crystallogr.* **1984**, *17*, 42–46.
(13) *International Tables for X-ray Crystallography*; Kynoch: Birmingham, England, 1974; Vol. IV, Tables 2.2A and 2.3.1.
(14) Ibers, J. A.; Hamilton, W. C. *Acta Crystallogr.* **1964**, *17*, 781–782.
(15) De Meulenaer, J.; Tompa, H. *Acta Crystallogr.* **1965**, *19*, 1014–1018.
(16) Tables III and IV have been deposited as supplementary material.
(17) Bjerkelund, E.; Kjekshus, A. *Acta Chem. Scand.* **1967**, *21*, 513–526.
(18) Bjerkelund, E.; Fermor, J. H.; Kjekshus, A. *Acta Chem. Scand.* **1966**, *20*, 1836–1842.

Table V. Bond Distances (Å) and Bond Angles (deg) in Ta_2MSe_7 (M = Pt, Ni)

dist	Ta_2NiSe_7	Ta_2PtSe_7	dist	Ta_2NiSe_7	Ta_2PtSe_7
Ta(1)–2Se(2)	2.600 (2)	2.615 (2)	Ta(1)–Se(6)	2.724 (2)	2.725 (4)
Ta(1)–2Se(5)	2.628 (2)	2.623 (2)	Ta(1)–Se(7)	2.725 (2)	2.745 (3)
Ta(1)–2Se(6)	2.630 (2)	2.646 (3)			
Ta(1)–Ta(1)	3.482 (1)	3.530 (3)			
Ta(2)–Se(3)	2.473 (2)	2.482 (3)	Ta(2)–2Se(1)	2.604 (2)	2.620 (2)
Ta(2)–2Se(4)	2.543 (2)	2.553 (2)	Ta(2)–Se(1)	2.720 (2)	2.700 (3)
Ta(2)–M	3.006 (3)	3.006 (2)	Ta(2)–Ta(2)	3.482 (1)	3.530 (3)
M–2Se(7)	2.394 (3)	2.490 (2)	M–Se(4)	2.467 (4)	2.589 (3)
M–2Se(3)	2.405 (3)	2.515 (2)	M–Se(2)	2.729 (4)	2.703 (3)
M–M	3.482 (1)	3.530 (3)			
Se(2)–Se(5)	2.549 (3)	2.597 (4)			
angle	**Ta_2NiSe_7**	**Ta_2PtSe_7**	**angle**	**Ta_2NiSe_7**	**Ta_2PtSe_7**
Se(2)–Ta(1)–Se(5)	58.36 (7)	59.45 (8)	Se(6)–Ta(1)–Se(6)	82.92 (7)	83.7 (1)
Se(2)–Ta(1)–Se(6)	145.60 (8)	144.90 (8)	Se(6)–Ta(1)–Se(7)	135.54 (8)	133.13 (9)
Se(1)–Ta(2)–Se(3)	169.88 (8)	162.95 (8)	Se(1)–Ta(2)–Se(4)	93.57 (5)	91.85 (8)
Se(1)–Ta(2)–Se(1)	83.94 (7)	84.7 (1)	Se(3)–Ta(2)–Se(4)	102.83 (7)	108.30 (8)
Se(3)–M–Se(7)	84.35 (6)	88.27 (8)	Se(4)–M–Se(7)	90.0 (1)	89.02 (8)
Se(3)–M–Se(7)	162.6 (2)	164.69 (8)	Se(3)–M–Se(3)	92.7 (1)	89.1 (1)
Se(3)–M–Se(4)	107.1 (1)	106.18 (8)	Se(7)–M–Se(7)	93.3 (1)	90.3 (1)

with that found in $TaSe_3$ (d = 2.576 (24) Å)[17] and are consistent with an intermediate Se–Se pair.[7]

For Ta_2NiSe_7 the average Ni–Se distance within the square pyramid is 2.413 (4) Å while the distance to the sixth Se atom in the octahedron is 2.729 (4) Å. This Ni coordination, while uncommon, is seen in both Ni_6Se_5[21] and $Ta_2Ni_3S_8$.[6] For Ta_2PtSe_7 the average Pt–Se distance in the square pyramid is 2.520 (3) Å while the distance to the sixth Se atom in the octahedron is 2.703 (3) Å. Thus, the Pt coordination, while still square pyramidal, is less distorted from octahedral geometry. The metrical details of the square-pyramidal site in these structures follow the same trends as those in $Ta_2Ni_3S_8$ and $Ta_2Pt_3Se_8$,[6] although in these compounds there is no sixth chalcogen atom in close proximity to the Ni or Pt atom. For example, the basal distances (M–Se(3) and M–Se(7), M = Ni or Pt) are somewhat shorter than the apical distance (M–Se(4)). Also, the metal atom lies above the basal plane of the square pyramid, resulting in an Se(3)–M–Se(7) angle that deviates from 180°. For Ta_2NiSe_7 this angle is 162.6 (2)°, and for Ta_2PtSe_7 it is 164.69 (8)°, in satisfactory agreement with the theoretical value of 164° for the C_{4v} square-pyramidal fragment ML_5, where M is a d^8 atom.[22]

The reason for this distortion to square-pyramidal geometry is not clear. However, it may be the consequence of an interaction between the M and Ta(2) atoms (M–Ta(2) = 3.006 (3) and 3.006 (2) Å for M = Ni and Pt, respectively). The highly asymmetric bonding between the Ta(2) atom and the apical atoms of the octahedron (e.g., Ta(2)–Se(1) = 2.720 (2) Å and Ta(2)–Se(3) = 2.473 (2) Å in Ta_2NiSe_7) may also result from such a metal–metal interaction.

The structure of Ta_2MSe_7 (M = Ni, Pt) is closely related to that of $FeNb_3Se_{10}$, which is presented in Figure 4. In $FeNb_3Se_{10}$ there are only two unique chains owing to disorder of Fe and Nb over the two octahedral sites. The chain of trigonal prisms is linked to the chain of octahedra through a different Se atom than are the chains in Ta_2NiSe_7. This difference in connectivity may be the origin of the shorter Se–Se bond in $FeNb_3Se_{10}$ (d = 2.348 (1) Å). In Ta_2MSe_7 one of the Se atoms in the Se–Se bond (Se(2)) belongs to the M octahedron as well as to the Ta trigonal prism. Furthermore, it is this same Se atom that is removed from the metal coordination sphere to give the square-pyramidal geometry about the M atom.

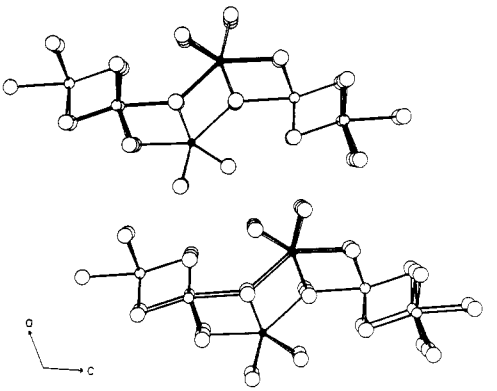

Figure 4. Perspective view of the $FeNb_3Se_{10}$ structure. Small filled circles are Nb atoms, small open circles are 50% Nb and 50% Fe atoms, and large open circles are Se atoms.

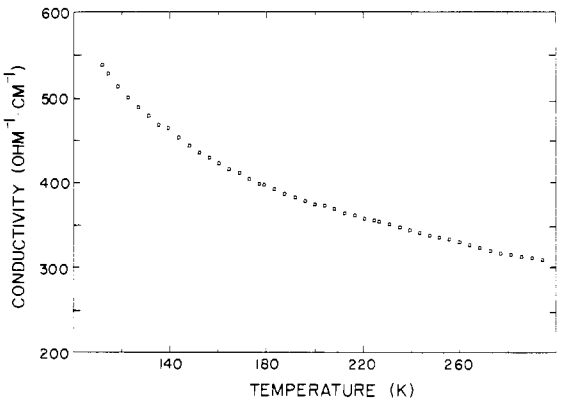

Figure 5. Plot of conductivity vs. temperature for single crystals of Ta_2NiSe_7 measured along the needle axis b.

Physical Properties. A plot of the temperature dependence of the magnetic susceptibility of Ta_2NiSe_7 between 1.8 and 290 K is given in Figure 5 (solid curve). The data can be corrected for paramagnetic impurities (μ_{eff} = 0.08 μ_B for the bulk sample) by fitting the results of low temperature (1.5–65 K) to the relation

$$\chi = \chi_0 + \frac{C}{T + \Theta}$$

where χ_0 is assumed to be temperature-independent at low T. The Curie–Weiss contribution ($C/(T + \Theta)$) is then subtracted from the data. The values of χ thus obtained are constant and negative

(19) Meerschaut, A. M.; Gressier, P.; Guemas, L.; Rouxel, J. *Mater. Res. Bull.* **1981**, *16*, 1035–1040.
(20) Cava, R. J.; Himes, V. L.; Mighell, A. D.; Roth, R. S. *Phys. Rev. B: Condens. Matter* **1981**, *24*, 3634–3637.
(21) Åkessson, G.; Røst, E. *Acta Chem. Scand., Ser. A* **1975**, *A29*, 236–240.
(22) Rossi, A. R.; Hoffmann, R. *Inorg. Chem.* **1975**, *14*, 365–374.

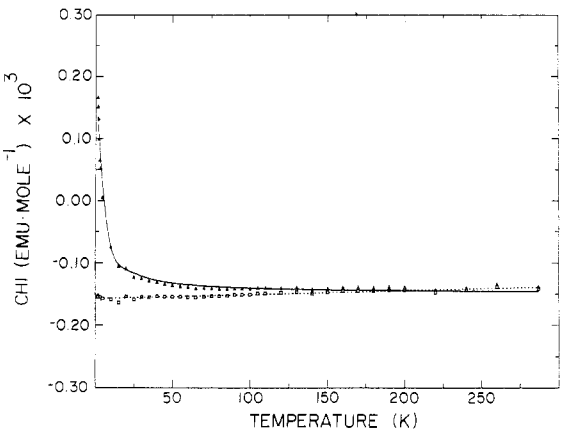

Figure 6. Plot of magnetic susceptibility vs. temperature for Ta_2NiSe_7: (solid line) raw data; (dashed line) data corrected for paramagnetic impurities.

(-1.54×10^{-7} emu g^{-1}) and are typical of a diamagnetic material (dashed curve in Figure 5). If, however, the data are corrected for ion-core diamagnetism,[23] the resulting susceptibility is small but positive (3.3×10^{-5} emu g^{-1}).

Four-probe single-crystal conductivity measurements along the needle axis, *b*, show that Ta_2NiSe_7 exhibits metallic behavior over the temperature range 100-300 K, with a room-temperature conductivity of 310 Ω^{-1} cm^{-1} (Figure 6). In this temperature range the material exhibits no metal-insulator transition as occurs at 140 K in $FeNb_3Se_{10}$.[24] The electrical conductivity is indicative of a material with a partially filled band at the Fermi level. Since the material is diamagnetic, the paramagnetism that arises from this partially filled band is small when compared with the ion-core diamagnetism. Because of the difficulty in obtaining large single crystals, the conductivity of the Pt compound has not been measured.

While Ta_2NiSe_7 has a structure similar to that of $FeNb_3Se_{10}$, the properties of these two compounds are very different and parallel those of the corresponding trichalcogenides. Thus, $FeNb_3Se_{10}$ is metallic and paramagnetic and displays charge density wave phenomena similar to those of $NbSe_3$,[25] while Ta_2NiSe_7 is metallic and diamagnetic and undergoes no phase transitions between 4 and 300 °C, analogous to the case for $TaSe_3$.[7]

Valence Description. It is difficult to describe these compounds in simple valence terms. The formal assignment $2Ta^{5+}M^{2+}$-$5Se^{2-}Se_2^{2-}$ is consistent with the single Se-Se bond evident in the structure. This description requires the Ta-centered bicapped trigonal prism that possesses the Se-Se bond to contain a Ta atom formally in the +5 state. To our knowledge all other Ta structures that contain Se-Se bonds are best described as having Ta^{4+} in the site with the chalcogen pair.[7,19] There may be some charge transfer from Se to Ta that leads to Ta^{4+} in the trigonal-prismatic site. Moreover, the majority of the Se-Se distances in the structure are between 3.1 and 3.6 Å, less than the sum of the ionic radii of two Se atoms (3.8 Å) but consistent with some extended Se-Se interactions. Thus, the metallic conduction could arise from Ta^{4+} in the bicapped-trigonal-prismatic sites, as occurs in $TaSe_3$.[7] This valence description ignores possible metal-metal interactions.

Conclusion

Attempts to extend the chemistry of the binary Nb and Ta trichalcogenides to ternary systems have led to the synthesis of the two new layered compounds Ta_2NiSe_7 and Ta_2PtSe_7. These compounds are isostructural. Their structure is similar to that of $FeNb_3Se_{10}$. The metallic conduction and diamagnetism of Ta_2NiSe_7 is similar to that of $TaSe_3$. The lack of charge density wave phenomena, which are observed in the structurally related compound $FeNb_3Se_{10}$, suggests that the physical properties of chalcogen-rich ternary chalcogenides parallel those of the corresponding binary trichalcogenides. The description of these compounds in terms of one-dimensional chains of metal atoms in consistent with the observed physical properties. This suggests that the hypothetical compounds Nb_2MSe_7 (M = Ni, Pd, Pt) might exhibit charge density wave phenomena. Attempts to synthesize such compounds have been unsuccessful to date.

Acknowledgment. This work was supported by the U.S. National Science Foundation, Solid State Chemistry (Grant DMR-83-15554). Some of the measurements were carried out in the SEM, X-ray, and magnetic susceptibility facilities of Northwestern University's Material Research Center, supported in part under the NSF-MRL program (Grant DMR82-16972).

Registry No. Ta_2NiSe_7, 104548-68-7; Ta_2PtSe_7, 104548-69-8; Ni, 7440-02-0; Pt, 7440-06-4; Ta, 7440-25-7; Se, 7782-49-2.

Supplementary Material Available: Anisotropic thermal parameters for Ta_2NiSe_7 (Table III) (1 page); structure amplitudes for both compounds (Table IV) (11 pages). Ordering information is given on any current masthead page.

(23) Klem, W. *Z. Anorg. Allg. Chem.* **1941**, *246*, 347-362.
(24) Hillenius, S. J.; Coleman, R. V.; Fleming, R. M.; Cava, R. J. *Phys. Rev. B: Condens. Matter* **1981**, *23*, 1567-1575.
(25) Bullet, D. W. *J. Phys. C* **1982**, *15*, 3069-3077.

Contribution from the Department of Chemistry, University of Vermont, Burlington, Vermont 05405

Oxidation-State-Dependent Changes in the Coordination Environment of Oxovanadium Complexes of Ethylenebis((*o*-hydroxyphenyl)glycine)

Joseph A. Bonadies and Carl J. Carrano*

Received January 27, 1986

Oxovanadium complexes of the ligand ethylenebis((*o*-hydroxyphenyl)glycine), EHPG, have been isolated and characterized with vanadium in both the +IV and +V oxidation states. Electrochemical study of these two complexes shows that they are interrelated as opposite corners of an ECEC square mechanism (E = electron-transfer step, C = chemical step). The mechanism was investigated in several solvents, and rates were determined for the chemical steps. An oxidation-state-dependent change in the coordination environments of the complexes was identified as the process occurring in the chemical steps of the mechanism.

Introduction

In order to better understand the interaction of vanadium with biological systems, the coordination chemistry of this element in its three accessible oxidation states (+III, +IV, and +V) with relevant ligands needs to be explored. In light of the reported binding of vanadium to the metal-tyrosinate protein transferrin[1] and its interaction with the recently characterized polyphenol tunichrome, found in the vanadocytes of the tunicates,[2] vanadi-

* To whom correspondence should be addressed.

(1) Harris, W. R.; Carrano, C. J. *J. Inorg. Biochem.* **1984**, *22*, 201.
(2) Bruening, R. C.; Oltz, E. M.; Furukawa, J.; Nakanishi, K.; Kustin, K. *J. Am. Chem. Soc.* **1985**, *107*, 5298.

0020-1669/86/1325-4358$01.50/0